

# **A Ray-Tracing Model for Cryogenic Target Uniformity Characterization**

**Sharon Jin**

# A Ray-Tracing Model for Cryogenic Target Uniformity Characterization

Sharon Jin

Advisor: Dr. Stephen Craxton

Laboratory for Laser Energetics

University of Rochester

Summer High School Research Program

2002

## Abstract

The Laboratory for Laser Energetics attempts to create fusion energy by irradiating a fuel capsule with many laser beams. In trying to achieve high energy gain, the fuel must be uniformly compressed to high density. Thus, the fuel capsule design is a thin plastic shell containing a thick layer of cryogenic Deuterium-Tritium (DT) fuel. One primary source of laser-fusion target performance degradation is a non-uniform inner surface on the dense fuel ice layer. Target characterization, therefore, uses shadowgraphy to produce within the periphery of the target image a virtual bright ring, a critical indication of variations in thickness of the fuel ice. A computer model, *Pegasus*, was built to trace light rays through an ideal target. It maps the outgoing intensity, taking into account Fresnel losses, polarization of light, ice absorption, and divergence of light path. In addition, the model sums up contributions from multiple light beams to allow finite F-numbers for both the light source and collection optics. Simulations of cryogenic and surrogate targets, when compared with experimental data, show agreement in intensity levels as well as in virtual bright ring position. This computer model aims to provide further insight into the best position of the focal plane, ideal combinations of light source and collection optics F-numbers, and effects of scattering on intensity.

## 1. Introduction

The ultimate goal of Inertial Confinement Fusion (ICF) research at the Laboratory for Laser Energetics (LLE) is to reap a high energy gain from fusion reactions with the OMEGA laser. In direct drive ICF, multiple, intense laser beams illuminate a spherical target pellet and compress it to extremely high plasma densities and temperatures [1].

By design, cryogenic targets are able to deliver a high concentration of fusion fuel. Cryogenic targets generally have a thin plastic (CH) shell, about  $3\mu\text{m}$ , enveloping a thick, dense layer of Deuterium ( $\text{D}_2$ ) or Deuterium-Tritium (DT) fuel, about  $100\mu\text{m}$ , chilled to 20K (see Fig. 1) [2,3].

The inner ice layer is formed by infrared radiation in  $\text{D}_2$  and beta heating in DT [4]. These methods currently make the layer uniform to  $3\mu\text{m}$  [5]. In order to achieve high energy gain, it is desirable to have uniformity to  $1\mu\text{m}$ , because any non-uniformity will grow exponentially under implosion conditions and decrease target performance.

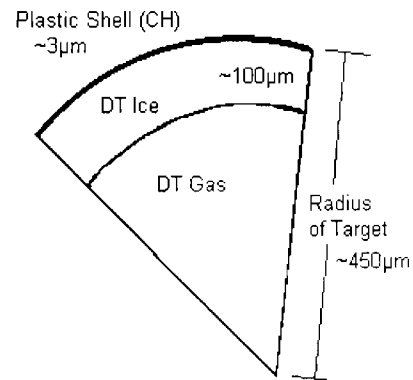
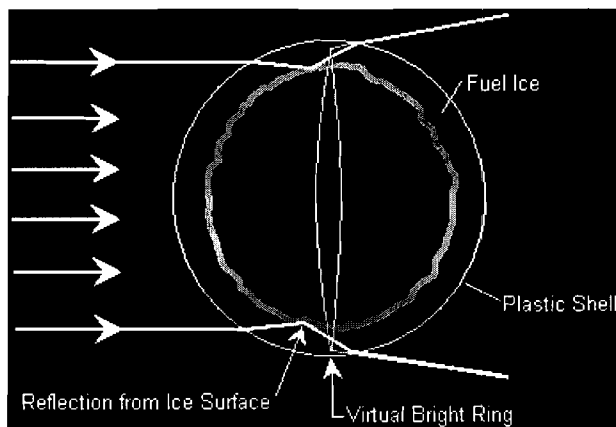


**Fig. 1:** Cross section of the cryogenic targets at LLE showing target component layers.

## 2. Shadowgraphy

Shadowgraphic analysis is a technique that characterizes inner ice surface non-



uniformities [4,6,7]. When a single collimated light source is shined on the target, the parallel light rays refract at the plastic shell and a few rays by total

**Fig. 2:** Experimental shadowgraphic analysis. Virtual bright ring shows inner ice uniformity.

internal reflection bounce off the inner ice surface as shown in Fig. 2. When these few rays are projected back to a focal plane, a virtual bright ring is formed. Deviations of this ring from a perfect circle as well as ring intensity give an accurate picture of the uniformity of the inner ice surface.

### 3. Ray Tracing Model *Pegasus*

This project involved writing a computer code, *Pegasus*, to model the experimental shadowgraphic system. *Pegasus* traces light rays through an ideal target and provides information on the position and intensity of the expected virtual bright ring. *Pegasus* can operate under two modes. One, it traces light rays from a single parallel light source. This portion of the code is based on an earlier ray tracing code [8]. Two, it incorporates multiple light beams from different directions in an effort to imitate real life conditions. The goal is to create a final intensity plot that will match up with experimental readouts from shadowgraphic analysis.

#### 3.1 Modeling ray paths in single beam ray tracing

The foundation of this project is using Snell's Law to trace the paths of light rays. First, the vectors which represent the light rays are defined, and thereafter, the position and direction of rays on the light path are calculated using vector algebra. The code starts with the desired number of rays from the light source plane with even intervals of height (see Fig. 3). These rays are each given a starting point and a direction. With this, the rays are then traced through every interface on the cryogenic target. The first surface is the thin plastic (CH) shell. Because light rays refract going from one medium to another medium of different density, Snell's Law must be used at this interface to find the new direction of the ray:

$$n_1 \sin \theta_i = n_2 \sin \theta_r$$

where  $\theta_i$  is the angle of incidence,  $n_1$  is the index of refraction for the first material,  $\theta_r$  is the angle of refraction,  $n_2$  and is the index for the second material. The index of refraction for the

first material, air in this case, is 1.00 and the index of refraction for the second material (plastic) is 1.59. The same principle is applied at each interface.

The code starts out with a large number of rays, but along the way, rays that do not fall into one of three predefined groups are terminated and therefore the graph only shows final intensity readouts for these three groups. At each successive interface, the code determines whether or not the ray intersects the next interface. The definition of each group is as follows:

- Group A rays must travel through all 6 interfaces: air-plastic, plastic-ice, ice-vapor, vapor-ice, ice-plastic, and plastic-air.
- Group B rays must reflect off the inner ice surface and follow this route: air-plastic, plastic-ice, reflect off inner ice surface, ice-plastic, plastic-air.
- Group C rays do not intersect the target at all and therefore do not use Snell's Law.

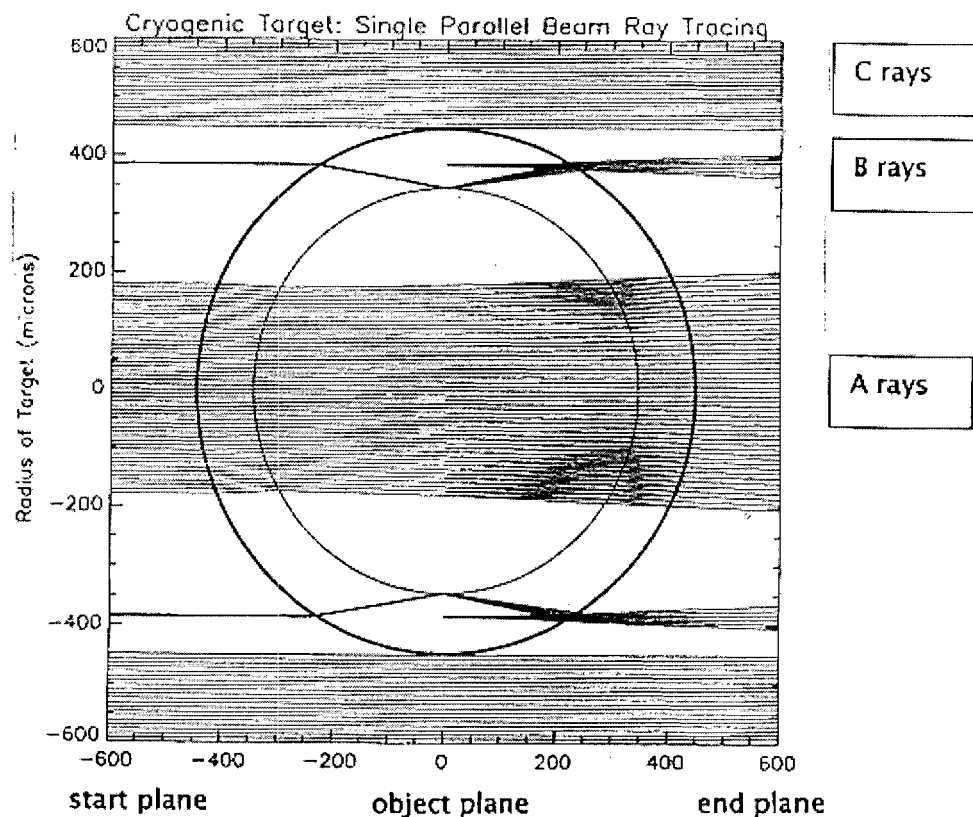


**Fig. 3:** Light rays are traced using Snell's Law through a cryogenic target of diameter 449 $\mu\text{m}$ . The axes represent distance in microns. The indices of refraction used for the interfaces were: air(1.00), plastic(1.59), ice(1.13), vapor(1.00). The object plane was placed at 0 $\mu\text{m}$ .

If a ray does not intersect the next interface, then it is tagged and the code aborts tracing its ray path. After each intersection with an interface, light rays have a new position vector and direction vector. Thus, the light rays are traced from a starting plane to an end plane then projected back to an object plane where intensity will be plotted.

### 3.2 Factors in calculating final intensity

Three major factors were considered in calculating final intensity. They are: Fresnel losses, ice absorption, and divergence of light path.

The Fresnel formulae are based on the physical phenomenon that when light travels from one medium to another of different refractive index, a portion of the light is transmitted while the rest is reflected back. The equations are as follows:

$$\text{Transmittance in p polarization} \quad T_p = \frac{2n_1 \cos \theta_i}{n_2 \cos \theta_i + n_1 \cos \theta_t}$$

$$\text{Transmittance in s polarization} \quad T_s = \frac{2n_1 \cos \theta_i}{n_1 \cos \theta_i + n_2 \cos \theta_t}$$

$$\text{Reflection in p polarization} \quad R_p = \frac{n_2 \cos \theta_i - n_1 \cos \theta_t}{n_2 \cos \theta_i + n_1 \cos \theta_t}$$

$$\text{Reflection in s polarization} \quad R_s = \frac{n_1 \cos \theta_i - n_2 \cos \theta_t}{n_1 \cos \theta_i + n_2 \cos \theta_t}$$

For the simulations shown in this report, the polarization was taken to be the average (A) of the p and s polarizations. The intensities after adjusting for Fresnel losses (where  $I_i$  is the initial intensity) are given as:

$$\text{Intensity after transmittance in p} \quad I_{Tp} = (n_2/n_1)(T_p)^2 I_i$$

$$\text{Intensity after transmittance in s} \quad I_{Ts} = (n_2/n_1)(T_s)^2 I_i$$

$$\text{Intensity after reflectance in p} \quad I_{Rp} = (R_p)^2 I_i$$

$$\text{Intensity after reflectance in s} \quad I_{Rs} = (R_s)^2 I_i$$

In the experimental readouts of a cryogenic target, it was observed that the A rays, particularly those passing through the center of the target without much refraction, ended up

with an intensity reduced to about 85% of the original intensities. This was accounted for by Fresnel losses.

Finally, intensity is defined as energy per area of space. The last major contributor to the final intensity plot accounted for by *Pegasus* is the divergence of the light path. The object plane is defined as a reference grid onto which light rays will be projected to map the final intensity. For each ray, the intensity is adjusted by the equation given below:

$$I_{\text{final}} = I_{\text{initial}} (\text{Area}_{\text{in}}/\text{Area}_{\text{out}})$$

where  $\text{Area}_{\text{in}}$  is taken to be the area between two neighboring rays at the starting plane and  $\text{Area}_{\text{out}}$  is taken to be the area between two neighboring rays at the object plane.

### 3.3 Diffuse illumination: multiple beams

In assuming a diffuse illumination, the source is represented as a large number of cylinders, pointed with various angles spread uniformly within the range of light defined by the initial f-number ( $F_{\text{in}}$ ). Light rays start from the source of illumination, but not all are collected by the end optic system. Only the light rays that fall within a set maximum collection angle contribute to the final intensity. The angles are given by the f-number of the illumination source and light collecting optic system:

$$\theta_{\text{inmax}} = \tan^{-1}(\frac{1}{2} F_{\text{in}})$$

$$\theta_{\text{outmax}} = \tan^{-1}(\frac{1}{2} F_{\text{out}})$$

This means the starting light rays must have angles to the propagation direction less than  $\theta_{\text{inmax}}$  to be traced through the target, and ending light rays must have angles less than  $\theta_{\text{outmax}}$  to be collected.

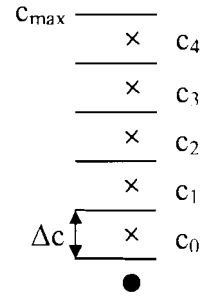
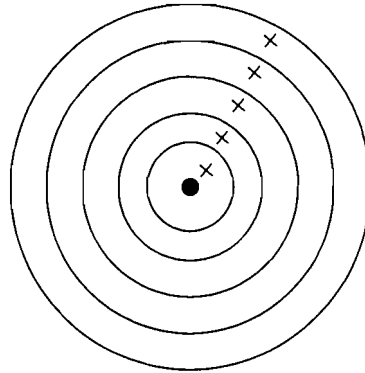
To account for the fact that the cylinders are spread uniformly in the input direction plane, the plane is divided into rings (see Fig. 4). The defining input direction for each ring is:

$$\Delta c = c_{\text{max}}/(\text{number of rings})$$

$$c_i = (1 + \frac{1}{2})\Delta c$$

Each ring is assigned an energy:  $E = (2c_i \Delta c)/(c_{\text{max}})$ , where Total Energy = 1. This gives the appropriate weight to each ring.

**Fig. 4:** Representation of diffuse light source as a series of cylinders of light, designated as weighted rings.



Each ring cylinder is divided into wedges and light rays from each wedge are traced through the target as in the single beam mode. To make the final intensity independent of the number of wedges, the initial intensity of each ray in the wedge was set to  $1/(\text{number of wedges})$ .

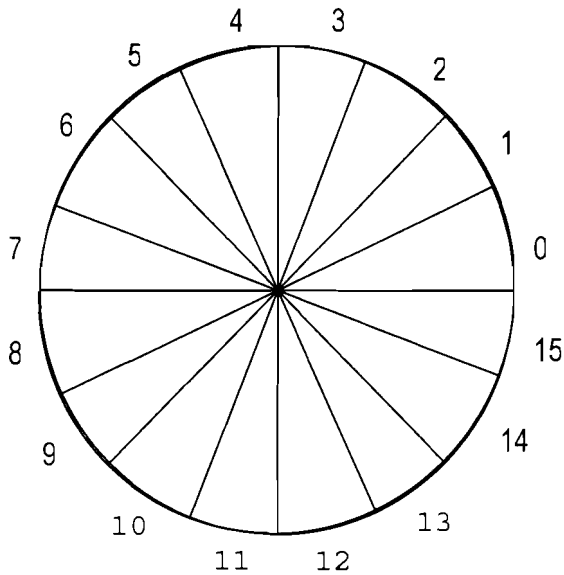


**Fig. 5:** A view of the incoming beam from the target center.

For  $i = 0 \dots (\text{number of wedges}) - 1$   
 $\Delta\theta = 2\pi / (\text{number of wedges})$   
 $\theta_{\text{wedge}(i)} = i (\Delta\theta)$

The angle of each wedge is used to assign a direction to each ray in the starting plane of the incoming beam.

Tracing light rays using a large number of rings and wedges results in an intensity graph that accurately reflects the conditions of experimental shadowgraphic analysis.

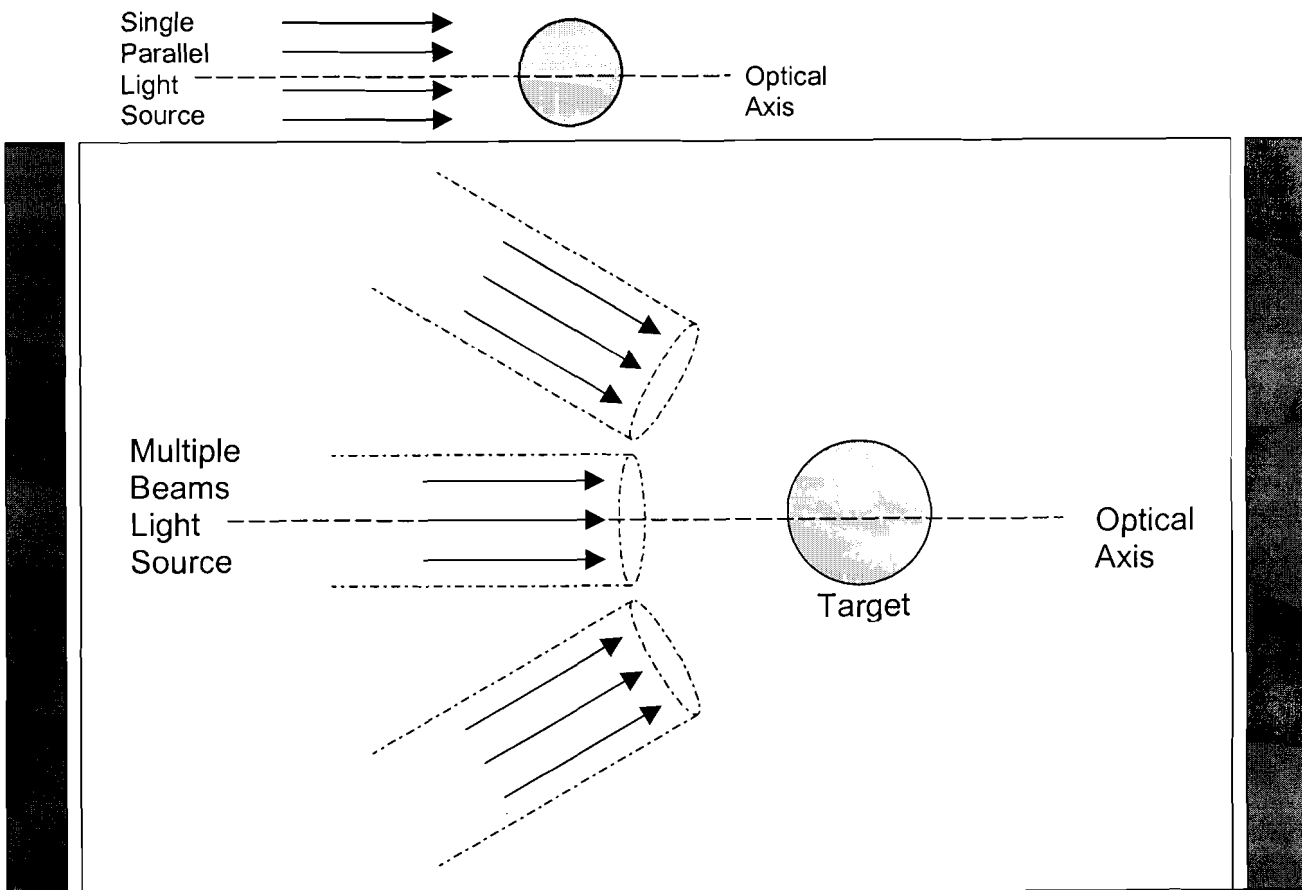


**Fig. 6:** *Pegasus* runs under two modes: single beam and multiple beam light tracing. Multiple beam light tracing is designed to closely resemble the experimental setup by the simulation of light from multiple directions.

### 3.4 Caustic Analysis

Caustic analysis specifically looks at the light rays that reflect off the inner ice surface and form the virtual bright ring. In this particular one dimensional, single beam trace of a cryogenic target, the caustic was located between 20 and 40 microns from the center vertical axis.

It is impossible experimentally to know where the focal plane is located to an accuracy of  $20\mu\text{m}$ . A small shift in the focal plane can result in a relatively large difference in intensity. In practice, the position of the focal plane can easily be varied when comparing with experimental data.

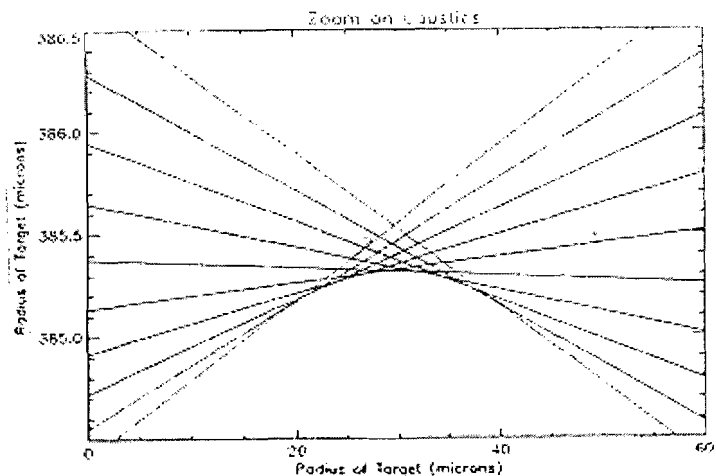


**Fig. 7:** Zoom of a portion of Fig. 3, where light rays converge when projected back to an object plane.

When running *Pegasus* initially, the focal plane was located at  $0\mu\text{m}$  on the horizontal axis. Adjustment of the focal plane position used by *Pegasus* would then be necessary after comparison with experimental data.

Because one of the major factors of final intensity is divergence of the light path, the location of the focal plane near a caustic, where light rays are very close together, can produce a very bright virtual ring. However, in real life, the ring is prevented from being infinitely bright by diffraction.

### 3.5 Intensity Comparisons

#### Cryogenic

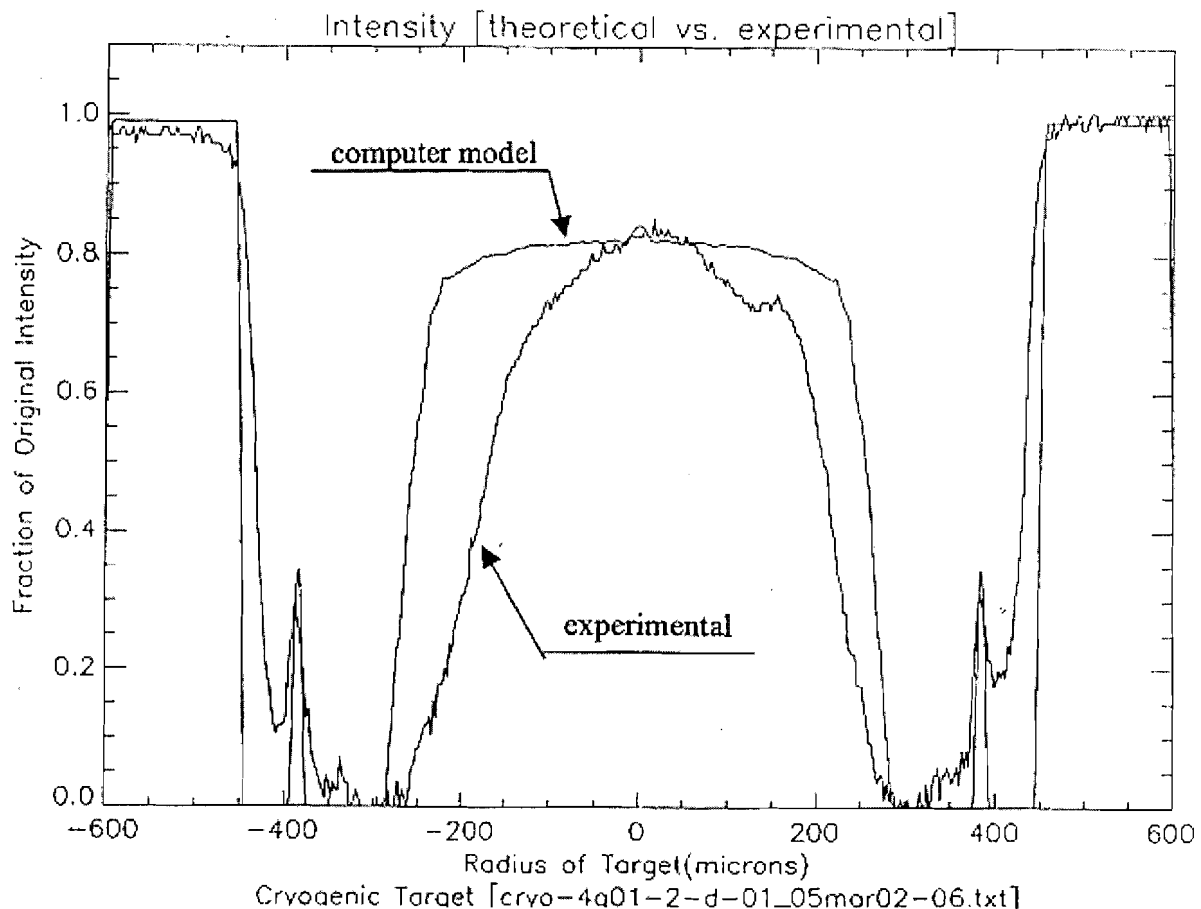


**Fig. 8:** An intensity comparison of the cryogenic target in Fig. 3. Final intensities are from experimental data and as modeled by *Pegasus*. The focal plane was located to  $-150\mu\text{m}$ .  $F_{in}$  was taken to be 5 and  $F_{out}$  12.

The intensity calculated by the modeling program *Pegasus* was superimposed onto intensity readouts from experimental shadowgraphic analysis, after scaling and interpolating onto a 1200-point reference grid (see Fig. 8). Here, the intensity was plotted for a cryogenic target of diameter 499 $\mu\text{m}$ . The center matches very well with the model, which had no absorption by the ice. The bright ring is observed at a radius of 380 $\mu\text{m}$  in both the computer model and experimental results. Because of caustic regions, the position of the focal plane has the greatest impact on the bright ring intensity. Placing the focal plane at -150 $\mu\text{m}$  brings model intensities close to experimental levels. The effects of scattering were not evaluated by *Pegasus* in these sets of simulations, which may account for the thinner experimental profile of A rays, and experimental intensity readings outside the 3 groups of rays this simulation analyzed.

#### Surrogate 1

Cryogenic targets are difficult to handle because of the fact that they must be kept chilled at 20K. In order to develop the characterization system more conveniently, representations are produced as surrogate targets. The surrogate target here is a thick plastic shell of a 650 $\mu\text{m}$  radius and about 190 $\mu\text{m}$  thickness. Light rays that form the bright ring in shadowgrams reflect off the inner surface of the plastic shell instead of the inner surface of the ice layer in cryogenic targets.

In Fig. 9, absorption by the thick plastic shell was taken in consideration by *Pegasus* and its effect is seen in the low center intensity. The bright ring is again modeled at the correct position. The width difference in the middle may be due to an experimental uncertainty in the F# actually used to collect the light.

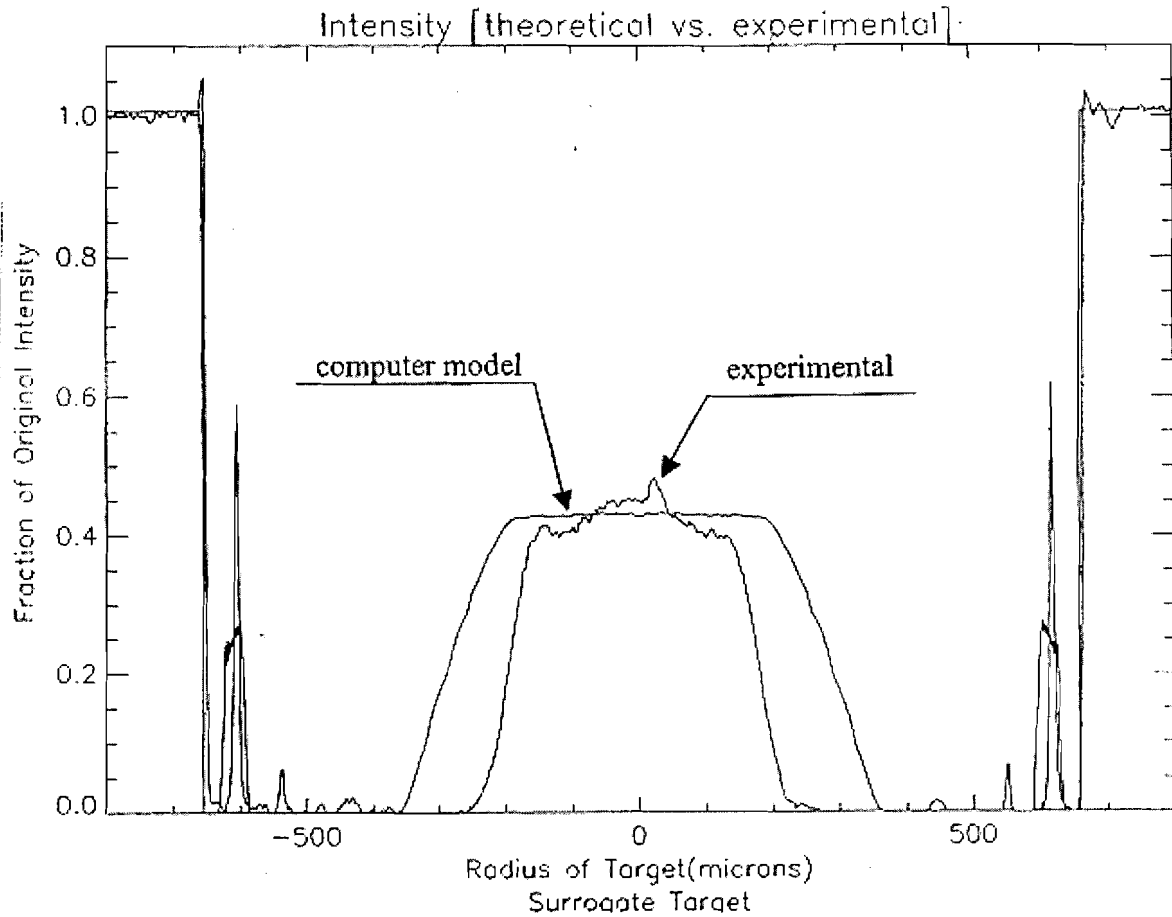


**Fig. 9:** An intensity comparison of a surrogate target. Final intensities are from experimental data and as modeled by *Pegasus*. The focal plane was located to  $24\mu\text{m}$ .  $F_{in}$  was taken to be 2.45 and  $F_{out}$  5.

The same surrogate target, under a different viewing system, produces a somewhat different intensity plot. The main difference between the two intensity plots is the F numbers, which sheds light on the large impact of the experimental setup on intensity data.

## Surrogate 2

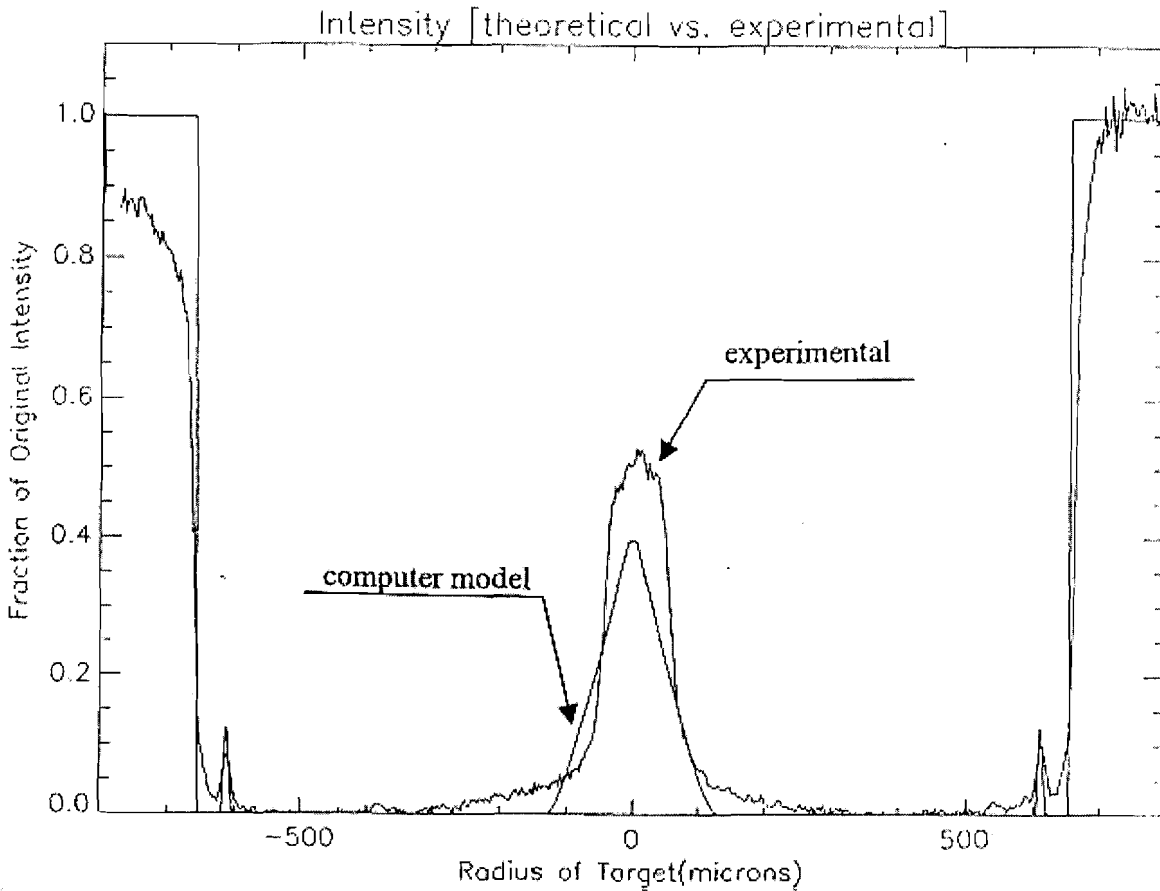


**Fig. 10:** An intensity comparison of the same surrogate target in Fig. 9 but under a different viewing system. Final intensities are from experimental data and as modeled by *Pegasus*. The focal plane was located to  $-100\mu\text{m}$ .  $F_{\text{in}}$  was taken to be 15 and  $F_{\text{out}}$  15.

In this case, the central portion is much thinner, probably because the collection optics had a larger F-number, or smaller angle through which rays were collected. *Pegasus* again correctly positioned the bright ring. The small level of experimental intensity readings in regions between the three groups modeled by *Pegasus* could be due to scattering of light rays, which presently is not accounted for by the computer model.

A comparison between Fig. 9 and Fig. 10 shows the tradeoff between a high F number and a low F number. Low F number has the advantage of a strong signal. High F number has the advantage of fewer rays collected and thus a narrower signal making it easier to accurately locate where the inner bright ring radius is.

## 5. Conclusions

A light tracing computer model *Pegasus* has been built to characterize cryogenic target uniformity. The OMEGA laser at LLE requires a highly uniform fuel layer surface, because non-uniformities will grow exponentially under Inertial Confinement Fusion and drastically reduce target performance. The code *Pegasus* has successfully modeled the paths of light rays from diffuse illumination through targets. Each layer in the cryogenic target has its respective index of refraction and this program follows the paths of 3 major groups of rays – A, B, and C – as they refract and reflect their way through. The B rays are the select few that reflect off the inner fuel layer surface. Where the B rays are projected back to meet the focal plane, a virtual bright ring is observed within the periphery of the target image in shadowgraphic analysis. It is the position, continuity, and intensity of this virtual bright ring that are analyzed to determine the uniformity of the inner ice surface.

By representing the uniform light source as rings and wedges, *Pegasus* traces each light ray through a target and then projects the light rays to an object plane where the intensity is plotted. The modeled intensity, when superimposed and compared with the experimental intensities, has shown strong agreement in intensity levels and position of virtual bright ring. The position of the focal plane has been shown to greatly affect bright ring intensities. This program is flexible so that input variables, such as thickness and index of refraction of each layer, collection optic F-number, and focal plane position, can be manipulated for modeling of future designs of Inertial Confinement Fusion targets.

## Acknowledgements

I would like to thank Dr. Stephen Craxton for giving me the opportunity to participate in the High School Summer Research program at the University of Rochester Laboratory for Laser Energetics, and for all the work he spent making the program so successful. I would also like to thank Dr. Craxton for working patiently with me for many hours and helping me through the project. A special thanks to all the other students in this program for the good times, and for becoming such important friends, especially my cubicle buddies! This has been one summer I will never forget.

## References

- [1] Craxton, R.S., Robert L. McCrory, and John M. Soures, *Scientific American*, Volume 225, pp. 68–79, “Progress in Laser Fusion (August 1986).”
- [2] Laboratory for Laser Energy Report LLE-02422, October 2001, Section 2.3, “Target Physics.”
- [3] Stoeckl et al., *LLE Review*, Volume 90, pp.49–56, January–March 2002, “First Results from Cryogenic Target Implosions on OMEGA.”
- [4] Bittner, D.N., et al., “Forming Uniform HD Layers in Shells Using Infrared Radiation,” *Fusion Technology*, Volume 35, March 1999, pp. 244–249.
- [5] Laboratory for Laser Energy Report LLE-02422, October 2001, Section 2.9, “Cryogenic Target Handling System.”
- [6] Sater, J., et al., General Atomics Report GA-A23240, FY99 ICF Annual Report, 5.1.2., “Shadowgraphy and Spherical Capsules.”
- [7] July 2001 Progress Report on the Laboratory for Laser Energetics Inertial Confinement Fusion Program Activities
- [8] Turner, Amy, “Ray Tracing Through the Liquid Crystal Point Diffraction Interferometer,” 1998 Summer High School Research Program at the University of Rochester’s Laboratory for Laser Energetics.